Inorg. Chem. **2004**, *43*, 1197–1205

Luminescent Heterotrinuclear Complexes with Pt(diimine)(dithiolate) and Metal Diphosphine as Components

Yan-Dan Chen,[†] Yong-Hai Qin,[†] Li-Yi Zhang,[†] Lin-Xi Shi,[†] and Zhong-Ning Chen*[,†,‡]

State Key Laboratory of Structural Chemistry, Fujian Institute of Research on the Structure of Matter, Chinese Academy of Sciences, Fuzhou, Fujian 350002, China, and State Key Laboratory of Coordination Chemistry, Nanjing University, Nanjing 210093, China

Received July 18, 2003

Reactions of Pt(diimine)(tdt) (tdt =3,4-toluenedithiolate) with $[M_2(dppm)_2(MeCN)_2]^{2+}$ (M = Cu^I or Ag^I, dppm = bis(diphenylphosphino)methane) gave heterotrinuclear complexes $[PtCu_2(tdt)(\mu\text{-SH})(dppm)_3](ClO_4)$ (**1**) and $[PtCu_2(diimine)_2(tdt)(dppm)_2](ClO_4)_2$ (diimine = 2,2′-bpyridine (bpy) **2**; 4,4′-dimethyl-2,2′-bipyridine (dmbpy) **3**; phenanthroline (phen) **4**, 5-bromophenanthroline (Brphen) **5**) for M = Cu^I, but $[PtAg_2(tdt)(\mu\text{-SH})(dppm)_3](SbF_6)$ (**6**) and $[PtAg_2(diimine)(tdt)(dppm)_2](SbF_6)_2$ (diimine = bpy **7**; dmbpy **8**; phen **9**; Brphen **10**) for M = Ag^I. While the complexes $[PtAg_2(diimine)(tdt)(dppm)_2](SbF_6)_2$ (**7**–**10**) result from linkage of Pt(diimine)(tdt) and $[M_2(dppm)_2(MeCN)_2]^{2+}$ by tdt sulfur donors, formation of $[PtCu_2(diimine)_2(tdt)(dppm)_2](ClO_4)_2$ (**2**–**5**) is related to rupture of metal–ligand bonds in the metal components and recombination between the ligands and the metal atoms by self-assembly. The formation of **1** and **6** is involved not only in dissociation and recombination of the metal components, but also in disruption of C–S bonds in the dithiolate (tdt). The dithiolate tdt adopts a chelating and bridging coordination mode in *anti* conformation for $[PtCu_2(diimine)_2(tdt)(dppm)_2](ClO_4)_2$ (**2**–**5**), whereas there is the *syn* conformation for other complexes. Compounds **1** and **6** represent sparse examples of μ-SH-bridged heterotrinuclear $Pt^{II}M^I_2$ complexes, in which Pt^{II}–M^I centers are bridged by dppm and sulfur donors of tdt, whereas M^I–M^I (M = Cu for **1**; Ag for **6**) centers are linked by dppm and the μ-SH donor. The ^{31}P NMR spectra show typical platinum satellites (J_{Pt-P} = 1450–1570 Hz) for **1**–**6** and Ag–P coupling for Pt^{II}–Ag^I (J_{Ag-P} = 350–450 Hz) complexes **6**–**10**. All of the complexes show intense emission in the solid state and in frozen glasses at 77 K. The complexes $[PtAg_2(diimine)(tdt)(dppm)_2](SbF_6)_2$ (**7**–**10**) also afford emission in fluid acetonitrile solutions at room temperature. Solid-state emission lifetimes at room temperature are in the microsecond range. It is revealed that emission energies of the trinuclear heterometallic complexes $[PtAg_2(diimine)(tdt)(dppm)_2](SbF_6)_2$ (**7**–**10**) exhibit a remarkable blue shift (0.10–0.35 eV) relative to those of the precursor compounds Pt(diimine)(tdt). The crystal structures of **1**, **2**, **4**, **6**, **8**, and **9** were determined by X-ray crystallography.

Introduction

The chemistry of transition metal diimine complexes is a subject of intensive interest owing to the applications of metal diimine chromophores in light-to-chemical energy conversion, luminescence sensors, and photonic molecular devices.[1–9] Recent research has been focused on square planar Pt^{II} diimine chromophores that can afford long-lived excited states and efficient photoluminescence.[10–22] Synthetic strat-

* To whom correspondence should be addressed. E-mail: czn@ms.fjirsm.ac.cn. Fax: +86-591-379-2346.

[†] Fujian Institute of Research on the Structure of Matter.

[‡] State Key Laboratory of Coordination Chemistry.

(1) (a) Paw, W.; Cummings, S. D.; Mansour, M. A.; Connick, W. B.; Geiger, D. K.; Eisenberg, R. *Coord. Chem. Rev.* **1998**, *171*, 125. (b) Hissler, M.; McGarrah, J. E.; Connick, W. B.; Geiger, D. K.; Cummings, S. D.; Eisenberg, R. *Coord. Chem. Rev.* **2000**, *208*, 115.

(2) Ziessel, R.; Hissler, M.; El-ghayoury, A.; Harriman, A. *Coord. Chem. Rev.* **1998**, *178*−*180*, 1251.

(3) (a) Chan, C. W.; Cheng, L. K.; Che, C. M. *Coord. Chem. Rev.* **1994**, *132*, 87. (b) Choi, M. Y.; Chan, M. C. W.; Peng, S. M.; Cheung, K. K.; Che, C. M. *Chem. Commun.* **2000**, 1259. (c) Lai, S. W.; Chan, M. C. W.; Cheung, K. K.; Che, C. M. *Organometallics* **1999**, *18*, 3327.

(4) (a) Yam, V. W. W.; Pui, Y. L.; Wong, K. M. C.; Cheung, K. K. *Chem. Commun.* **2000**, 1751. (b) Yam, V. W. W.; Yang, Y.; Zhang, J.; Chu, B. W. K.; Zhu, N. *Organometallics* **2001**, *20*, 4911. (c) Yam, V. W. W.; Chong, S. H. F.; Wong, K. M. C.; Cheung, K. K. *Chem. Commun.* **1999**, 1013. (d) Yam, V. W. W.; Wong, K. M. C.; Chong, S. H. F.; Lau, V. C. Y.; Lam, S. C. F.; Zhang, L.; Cheung, K. K. *J. Organomet. Chem.* **2003**, *670*, 205.

(5) Smucker, B. W.; Hudson, J. M.; Omary, M. A.; Dunbar, K. R. *Inorg. Chem.* **2003**, *42*, 4714.

10.1021/ic034848a CCC: $27.50
Published on Web 01/07/2004

egy is aimed not only at understanding the molecular factors that govern the excited state properties by systematic variations in square planar Pt^{II} diimine chromophores, but also at developing diad, triad, and multicomponent systems based on Pt(diimine)(dithiolate)[14−17] or Pt(diimine)(acetylide)[10−13] components for more efficient photoluminescence and for electronic devices capable of energy conversion and storage.

In order to attain luminescent heterometallic molecular materials, an efficient approach is to utilize two types of metal components capable of incorporation to each other by self-assembly.[23] In view of potentially bridging character of the sulfur donors in Pt(diimine)(dithiolate), we are interested in developing multicomponent systems based on square planar Pt^{II} diimine chromophores by incorporating them into another metal component with vacant or substitutable coordination sites. As the first step in our synthetic strategy for luminescent heterometallic assemblies based on Pt^{II} diimine chromophores, the self-assembly reactions between Pt(diimine)(dithiolate) and $[M_2(\mu\text{-dppm})_2(MeCN)_2]^{2+}$ were investigated and described herein.

Experimental Section

Material and Reagents. (**Caution!** Perchlorate salts are potentially explosive and should be handled with care and in small amounts.) All synthetic operations were performed under dry argon atmosphere by using Schlenk techniques. Solvents were dried by standard methods and distilled prior to use. The reagents potassium tetrachloroplatinum ($K_2[PtCl_4]$), 3,4-toluenedithiol (H_2tdt), bis(diphenylphospino)methane (dppm), silver hexafluoroantimonate ($AgSbF_6$), 2,2′-bipyridine (bpy), 4,4-dimethyl-2,2′-bipyridine (dmbpy), and 1,10-phenanthroline (phen) were commercial available (from Acros, Fluka, Alfa Aesar, or Aldrich Chemical Co.). 5-Bromophenanthroline (Brphen) was prepared according to literature methods.[10d] The compounds Pt(bpy)Cl_2, Pt(dmbpy)Cl_2, Pt(phen)Cl_2, and Pt(Brphen)Cl_2 were prepared by the described procedures.[24] The compounds $[Cu_2(dppm)_2(MeCN)_2](ClO_4)_2$,[25a] $[Ag_2(dppm)_2(MeCN)_2](SbF_6)_2$,[25b] and Pt(diimine)(tdt) (diimine = bpy, dmbpy, phen, and Brphen)[15] were prepared by similar synthetic procedures described in the literature.

$[PtCu_2(tdt)(\mu\text{-SH})(dppm)_3](ClO_4)$ (1) and $[PtCu_2(bpy)_2(tdt)(dppm)_2](ClO_4)_2$ (2). To a dichloromethane (20 mL) solution of Pt(bpy)(tdt) (50.5 mg, 0.10 mmol) was added $[Cu_2(dppm)_2(MeCN)_2](ClO_4)_2$ (117.7 mg, 0.10 mmol) to give an orange solution. After the solution was stirred at room temperature for 1 day, it was filtered to remove a little precipitate. The filtrate was then concentrated in vacuo to leave 3 mL in volume and chromatographed on a silica gel column. Elution of the solution with dichloromethane afforded a bit of sample in the first band which was identified as the starting material Pt(bpy)(tdt). Complex **1** was eluted with dichloromethane−acetone (v/v 20:1) as the second band to give 15 mg of the pale yellow product. Yield: 8%. Complex **2** was eluted with dichloromethane−acetone (v/v 6:1) as the third band to give 86 mg of the yellow product. Yield: 46%.

Compound 1. Anal. Calcd for $C_{82}H_{73}ClO_4P_6S_3Cu_2Pt\cdot{}^1/_2CH_2Cl_2\cdot{}^1/_2CH_3OH$: C, 54.81; H, 4.22. Found: C, 54.73; H, 4.24. ES-MS (*m*/*z*): 1664 ($[M - ClO_4]^+$), 1280 ($[PtCu_2(tdt)(\mu\text{-SH})(dppm)_2]^+$), 1181 ($[PtCu(tdt)(dppm)_2]^+$), 895 ($[PtCu_2(tdt)(\mu\text{-SH})(dppm)]^+$). IR spectrum (KBr, cm^{-1}): ν 1095 (s, ClO_4). ^{31}P NMR spectrum (202.3 MHz, CD_3CN, ppm): δ 5.6 (d, $CuPCH_2PPt$, $J_{Pt-P} = 1570$ Hz, $^2J_{P-P} = 43$ Hz), −11.6 (s, $CuPCH_2PPt$), −17.6 (s, $CuPCH_2PCu$).

Compound 2. Anal. Calcd for $C_{77}H_{66}Cl_2Cu_2N_4O_8P_4PtS_2\cdot{}^3/_2CH_2Cl_2$: C, 50.13; H, 3.70; N, 2.98. Found: C, 49.82; H, 4.13; N, 2.91. ES-MS (*m*/*z*): 1181 ($[PtCu(tdt)(dppm)_2]^+$), 778 ($[M - (ClO_4)_2]^{2+}$), 700 ($[PtCu_2(bpy)(tdt)(dppm)_2]^{2+}$), 619 ($[PtCu_2(tdt)(dppm)_2]^{2+}$). IR spectrum (KBr, cm^{-1}): ν 1095 (s, ClO_4). ^{31}P NMR spectrum (202.3 MHz, CD_3CN, ppm): δ 6.9 (s, $CuPCH_2PPt$, $J_{Pt-P} = 1468$ Hz), −17.6 (s, $CuPCH_2PPt$).

(6) (a) Riesgo, E. C.; Hu, Y. Z.; Bouvier, F.; Thummel, R. P.; Scaltrito, D. V.; Meyer, G. J. *Inorg. Chem.* **2001**, *40*, 3413. (b) Hu, Y. Z.; Xiang, Q.; Thummel, R. P. *Inorg. Chem.* **2002**, *41*, 3423. (c) Wu, F.; Riesgo, E.; Pavalova, A.; Kipp, R. A.; Schmehl, R.; Thummel, R. P. *Inorg. Chem.* **1999**, *38*, 5620. (d) Jahng, Y.; Hazelrigg, J.; Kimball, D.; Riesgo, E.; Wu, F.; Thummel, R. P. *Inorg. Chem.* **1997**, *36*, 5390.

(7) Meyer, M.; Albrecht-Gary, A. M.; Dietrich-Buchecker, C. O.; Sauvage, J. P. *Inorg. Chem.* **1999**, *38*, 2279.

(8) (a) Kuang, S. M.; Cuttell, D. G.; McMillin, D. R.; Fanwick, P. E.; Walton, R. A. *Inorg. Chem.* **2002**, 41, 3313. (b) Cunningham, C. T.; Moore, J. J.; Cunningham, K. L. H.; Fanwick, P. E.; McMillin, D. R. *Inorg. Chem.* **2000**, *39*, 3638. (c) Cunningham, C. T.; Cunningham, K. L. H.; Michalec, J. F.; McMillin, D. R. *Inorg. Chem.* **1999**, *38*, 4388. (d) Cuttell, D. G.; Kuang, S. M.; Fanwick, P. E.; McMillin, D. R.; Walton, R. A. *J. Am. Chem. Soc.* **2002**, *124*, 6.

(9) (a) Miller, M. T.; Gantzel, P. K.; Karpishin, T. B. *J. Am. Chem. Soc.* **1999**, *121*, 4292. (b) Miller, M. T.; Karpishin, T. B. *Inorg. Chem.* **1999**, *38*, 5246. (c) Miller, M. T.; Gantzel, P. K.; Karpishin, T. B. *Inorg. Chem.* **1999**, *38*, 3414. (d) Miller, M. T.; Gantzel, P. K.; Karpishin, T. B. *Inorg. Chem.* **1998**, *37*, 2285.

(10) (a) McGarrah, J. E.; Eisenberg, R. *Inorg. Chem.* **2003**, *42*, 4355. (b) Wadas, T. J.; Lachicotte, R. J.; Eisenberg, R. *Inorg. Chem.* **2003**, *42*, 3772. (c) McGarrah, J. E.; Kim, Y. J.; Hissler, M.; Eisenberg, R. *Inorg. Chem.* **2001**, *40*, 4510. (d) Hissler, M.; Connick, W. B.; Geiger, D. K.; McGarrah, J. E.; Lipa, D.; Lachicotte, R. J.; Eisenberg, R. *Inorg. Chem.* **2000**, *39*, 447.

(11) Chan, S. C.; Chan, M. C. W.; Wang, Y.; Che, C. M.; Cheung, K. K.; Zhu, N. *Chem. Eur. J.* **2001**, *7*, 4180.

(12) Pomestchenko, I. E.; Luman, C. R.; Hissler, M.; Ziessel, R.; Castellano, F. N. *Inorg. Chem.* **2003**, *42*, 1394.

(13) Whittle, C. E.; Weinstein, J. A.; George, M. W.; Schanze, K. S. *Inorg. Chem.* **2001**, *40*, 4053.

(14) (a) Tzeng, B. C.; Chan, S. C.; Chan, M. C. W.; Che, C. M.; Cheung, K. K.; Peng, S. M. *Inorg. Chem.* **2001**, *40*, 6699. (b) Tzeng, B. C.; Fu, W. F.; Che, C. M.; Chao, H. Y.; Cheung, K. K.; Peng, S. M. *J. Chem. Soc., Dalton Trans.* **1999**, 1017.

(15) (a) Cummings, S. D.; Eisenberg, R. *J. Am. Chem. Soc.* **1996**, *118*, 1949. (b) Zuleta, J. A.; Chesta, C. A.; Eisenberg, R. *J. Am. Chem. Soc.* **1989**, *111*, 8916. (c) Zuleta, J. A.; Bevilacqua, J. M.; Proserpio, D. M.; Harvey, P. D.; Eisenberg, R. *Inorg. Chem.* **1992**, *31*, 2396. (d) Cummings, S. D.; Eisenberg, R. *Inorg. Chem.* **1995**, *34*, 2007. (e) Bevilacqua, J. M.; Eisenberg, R. *Inorg. Chem.* **1994**, *33*, 1886. (f) Zuleta, J. A.; Bevilacqua, J. M.; Rehm, J. M.; Eisenberg, R. *Inorg. Chem.* **1992**, *31*, 1332. Bevilacqua, J. M.; Eisenberg, R. *Inorg. Chem.* **1994**, *33*, 2913. (g) Huertas, S.; Hissler, M.; McGarrah, J. E.; Lachicotte, R. J.; Eisenberg, R. *Inorg. Chem.* **2001**, *40*, 1183. (h) Paw, W.; Connick, W. B.; Eisenberg, R. *Inorg. Chem.* **1998**, *37*, 3919. (i) Paw, W.; Lachicotte, R. J.; Eisenberg, R. *Inorg. Chem.* **1998**, *37*, 4139.

(16) Kato, M.; Omura, A.; Toshikawa, A.; Kishi, S.; Sugimoto, Y. *Angew. Chem., Int. Ed.* **2002**, *41*, 3183.

(17) Connick, W. B.; Gray, H. B. *J. Am. Chem. Soc.* **1997**, *119*, 11620.

(18) Cocker, T. M.; Bachman, R. E. *Inorg. Chem.* **2001**, *40*, 1550.

(19) Connick, W. B.; Miskowski, V. M.; Houlding, V. H.; Gray, H. B. *Inorg. Chem.* **2000**, *39*, 2585.

(20) (a) Zheng, G. Y.; Rillema, D. P.; DePriest, J.; Woods, C. *Inorg. Chem.* **1998**, *37*, 3588. (b) DePriest, J.; Zheng, G. Y.; Goswami, N.; Eichhorn, D. M.; Woods, C.; Rillema, D. P. *Inorg. Chem.* **2000**, *39*, 1955. (c) Wang, Y.; Perez, W.; Zheng, G. Y.; Rillema, D. P. *Inorg. Chem.* **1998**, *37*, 2051.

(21) Fanizzi, F. P.; Natile, G.; Lanfranchi, M.; Tiripicchio, A.; Laschi, F.; Zanello, P. *Inorg. Chem.* **1996**, *35*, 3173.

(22) Dungey, K. E.; Thompson, B. D.; Kane-Maguire, N. A. P.; Wright, L. L. *Inorg. Chem.* **2000**, *39*, 5192.

(23) (a) Xu, H. W.; Chen, Z. N.; Ishizaka, S.; Kitamura, N.; Wu, J. G. *Chem. Commun.* **2002**, 1934. (b) Wei, Q. H.; Yin, G. Q.; Ma, Z.; Shi, L. X.; Chen, Z. N. *Chem. Commun.* **2003**, 2188.

(24) Hodges, K. D.; Rund, J. V. *Inorg. Chem.* **1975**, *14*, 525.

(25) (a) Diez, J.; Gamasa, M. P.; Gimeno, J.; Tiripicchio, A.; Camellini, M. T. *J. Chem. Soc., Dalton Trans.* **1987**, 1275. (b) Ho, D. M.; Bau, R. *Inorg. Chem.* **1983**, *22*, 4073.

[PtCu$_2$(dmbpy)$_2$(tdt)(dppm)$_2$](ClO$_4$)$_2$ (3). The reaction was carried out in the same procedure as the synthesis of **2** using Pt(dmbpy)(tdt) instead of Pt(bpy)(tdt) to give 65 mg of a yellow product. Yield: 34%. Anal. Calcd for $C_{81}H_{74}Cl_2Cu_2N_4O_8P_4PtS_2 \cdot CH_2Cl_2$: C, 51.90; H, 4.04; N, 2.95. Found: C, 51.67; H, 3.79; N, 2.94. ES-MS (*m*/*z*): 1713 ([M − (ClO$_4$)]$^+$), 1527 ([PtCu$_2$(dmbpy)(tdt)(dppm)$_2$(ClO$_4$)]$^+$), 1181 ([PtCu(tdt)(dppm)$_2$]$^+$), 863 ([Pt(dmbpy)(dppm)(ClO$_4$)]$^+$), 807 ([M − (ClO$_4$)$_2$]$^{2+}$), 714 ([PtCu$_2$(dmbpy)(tdt)(dppm)$_2$]$^{2+}$), 650 ([Cu$_2$(dmbpy)$_2$(tdt)]$^+$), 633 ([Pt(dmbpy)(tdt)(ClO$_4$)]$^+$). IR spectrum (KBr, cm^{-1}): ν 1092 (s, ClO$_4$). ^{31}P NMR spectrum (202.3 MHz, CD$_3$CN, ppm): δ 8.5 (s, CuPCH$_2$*P*Pt, J_{Pt-P} = 1517 Hz), −16.0 (s, Cu*P*CH$_2$PPt).

[PtCu$_2$(phen)$_2$(tdt)(dppm)$_2$](ClO$_4$)$_2$ (4). The same procedure as that for **2** was applied except that Pt(phen)(tdt) was used instead of Pt(bpy)(tdt) to afford 74 mg of a yellow product. Yield: 39%. Anal. Calcd for $C_{81}H_{66}Cl_2N_4O_8P_4S_2Cu_2Pt \cdot CH_2Cl_2$: C, 52.13; H, 3.63; N, 2.97. Found: C, 52.19; H, 3.75; N, 2.96. ES-MS (*m*/*z*): 1705 ([M − (ClO$_4$)]$^+$), 1359 ([PtCu(phen)(tdt)(dppm)$_2$]$^+$), 1181 ([PtCu(tdt)(dppm)$_2$]$^+$), 976 ([PtCu(phen)(tdt)(dppm)]$^+$), 802 ([M − (ClO$_4$)$_2$]$^{2+}$), 413 ([PtCu(tdt)]$^+$), 352 ([Pt(tdt)]$^+$). IR spectrum (KBr, cm^{-1}): ν 1095 (s, ClO$_4$). ^{31}P NMR spectrum (202.3 MHz, CD$_3$CN, ppm): δ 8.9 (t, CuPCH$_2$*P*Pt, J_{Pt-P} = 1470 Hz, $^2J_{P-P}$ = 55 Hz), −14.9 (s, Cu*P*CH$_2$PPt).

[PtCu$_2$(Brphen)$_2$(tdt)(dppm)$_2$](ClO$_4$)$_2$ (5). The synthetic procedure was the same as that for **2** except that Pt(Brphen)(tdt) was used instead of Pt(bpy)(tdt) to afford 63 mg of an orange-yellow product. Yield: 32%. Anal. Calcd for $C_{81}H_{64}Br_2Cl_2N_4O_8P_4S_2Cu_2Pt$: C, 49.58; H, 3.29; N, 2.86. Found: C, 49.92; H, 3.27; N, 2.60. ES-MS (*m*/*z*): 1863 ([M − (ClO$_4$)]$^+$), 1441 ([PtCu(Brphen)(tdt)(dppm)$_2$]$^+$), 1181 ([PtCu(tdt)(dppm)$_2$]$^+$), 882 ([M − (ClO$_4$)$_2$]$^{2+}$), 623 ([PtCu$_2$(tdt)(dppm)$_2$]$^{2+}$). IR spectrum (KBr, cm^{-1}): ν 1095 (s, ClO$_4$).^{31}P NMR spectrum (202.3 MHz, CD$_3$CN, ppm): δ 8.8 (d, CuPCH$_2$*P*Pt, J_{Pt-P} = 1457 Hz, $^2J_{P-P}$ = 73 Hz), −14.5 (s, Cu*P*CH$_2$PPt).

[PtAg$_2$(tdt)(μ-SH)(dppm)$_3$](SbF$_6$) (6) and [PtAg$_2$(bpy)(tdt)(dppm)$_2$](SbF$_6$)$_2$ (7). To a dichloromethane (10 mL) solution of Pt(bpy)(tdt) (50.5 mg, 0.10 mmol) was added a dichloromethane (5 mL) suspended solution of [Ag$_2$(dppm)$_2$(MeCN)$_2$](SbF$_6$)$_2$ (153.8 mg, 0.10 mmol) to afford a clear red-orange solution. It was stirred at room temperature for 12 h to produce a yellow precipitate. The solvent was then removed in vacuo, and the residue was dissolved in 5 mL of acetonitrile to afford a red solution. It was then chromatograghed on a silica gel column using dichloromethane−acetonitrile (v/v 8:1) as an eluent to afford **6** (11 mg, yield 5%) and **7** (147 mg, yield 75%) in the first and second bands, respectively.

Compound 6. Anal. Calcd for $C_{82}H_{73}F_6P_6S_3SbAg_2Pt \cdot CH_2Cl_2$: C, 48.11; H, 3.65. Found: C, 48.43; H, 3.42. ES-MS (*m*/*z*): 1752 ([M − (SbF$_6$)]$^+$), 1369 ([PtAg$_2$(tdt)(μ-SH)(dppm)$_2$]$^+$), 1225 ([PtAg(tdt)(dppm)$_2$]$^+$), 983 ([PtAg$_2$(tdt)(μ-SH)(dppm)]$^+$). ^{31}P NMR spectrum (202.3 MHz, CD$_3$CN, ppm): δ 6.3 (d, AgPCH$_2$*P*Pt, $^1J_{Pt-P}$ = 1450 Hz, $^2J_{P-P}$ = 55 Hz), −2.5 (d, Ag*P*CH$_2$PPt, J_{Ag-P} = 439 Hz), −13.6 (d, Ag*P*CH$_2$PAg, J_{Ag-P} = 355 Hz).

Compound 7. Anal. Calcd for $C_{67}H_{58}N_2F_{12}P_4S_2Sb_2Ag_2Pt$: C, 41.03; H, 2.98; N, 1.43. Found: C, 40.94; H, 2.56; N, 1.60. ES-MS (*m*/*z*): 1725 ([M − (SbF$_6$)]$^+$), 1341 ([PtAg$_2$(bpy)(tdt)(dppm)(SbF$_6$)]$^+$), 997 ([PtAg(bpy)(tdt)(dppm)]$^+$), 745 ([M − (SbF$_6$)$_2$]$^{2+}$), 666 ([PtAg$_2$(tdt)(dppm)$_2$]$^{2+}$), 491 ([Ag$_2$(dppm)$_2$]$^{2+}$). IR spectrum (KBr, cm^{-1}): ν 660 (s, SbF$_6$). ^{31}P NMR spectrum (202.3 MHz, CD$_3$CN, ppm): δ 5.3 (d, J_{Ag-P} = 436 Hz).

[PtAg$_2$(dmbpy)(tdt)(dppm)$_2$](SbF$_6$)$_2$ (8). It was prepared by the same procedure as **7** using Pt(dmbpy)(tdt) instead of Pt(bpy)(tdt) to give 150.0 mg of **8** as a yellow solid. Yield: 75%. Anal. Calcd for $C_{69}H_{62}N_2F_{12}P_4S_2Sb_2Ag_2Pt$: C, 41.66; H, 3.14; N, 1.41. Found: C, 41.54; H, 3.02; N, 1.48. ES-MS (*m*/*z*): 1752 ([M − (SbF$_6$)]$^+$), 1369 ([PtAg$_2$(dmbpy)(tdt)(dppm)](SbF$_6$)$^+$), 1025 ([PtAg(dmbpy)(tdt)(dppm)]$^+$), 985 ([PtAg$_2$(dmbpy)(tdt)(SbF$_6$)]$^+$), 759 ([M − (SbF$_6$)$_2$]$^{2+}$), 666 ([PtAg$_2$(tdt)(dppm)$_2$]$^{2+}$), 493 ([Ag$_2$(dppm)$_2$]$^{2+}$). IR spectrum (KBr, cm^{-1}): ν 660 (s, SbF$_6$). ^{31}P NMR spectrum (202.3 MHz, CD$_3$CN, ppm): δ 4.7 (d, J_{Ag-P} = 427 Hz).

[PtAg$_2$(phen)(tdt)(dppm)$_2$](SbF$_6$)$_2$ (9). The preparation was the same as that for complex **7** using Pt(phen)(tdt) instead of Pt(bpy)(tdt) to give an orange-yellow product. Yield: 60%. Anal. Calcd for $C_{69}H_{58}N_2F_{12}P_4S_2Sb_2Ag_2Pt$: C, 41.74; H, 2.94; N, 1.41. Found: C, 41.55; H, 2.80; N, 1.49. IR spectrum (KBr, cm^{-1}): ν 660 (s, SbF$_6$). ES-MS (*m*/*z*): 1749 ([M − (SbF$_6$)]$^+$), 1547 ([PtAg$_2$(phen)$_2$(tdt)(dppm)](SbF$_6$)$^+$), 1021 ([PtAg(phen)(tdt)(dppm)]$^+$), 757 ([M − (SbF$_6$)$_2$]$^{2+}$), 491 ([Ag$_2$(dppm)$_2$]$^{2+}$). ^{31}P NMR spectrum (202.3 MHz, CD$_3$CN, ppm): δ 5.3 (d, J_{Ag-P} = 427 Hz).

[PtAg$_2$(Brphen)(tdt)(dppm)$_2$](SbF$_6$)$_2$ (10). The preparation was similar to that for complex **7** using [Pt(Brphen)(tdt)] instead of Pt(bpy)(tdt) to give an orange-red product. Yield: 60%. Anal. Calcd for $C_{69}H_{57}N_2F_{12}P_4S_2BrSb_2Ag_2Pt \cdot CH_2Cl_2$: C, 39.12; H, 2.77; N, 1.30. Found: C, 39.26; H, 2.55; N, 1.36. IR spectrum (KBr, cm^{-1}): ν 660 (s, SbF$_6$). ES-MS (*m*/*z*): 1826 ([M − SbF$_6$]$^+$), 1443 ([PtAg$_2$(Brphen)(tdt)(dppm)(SbF$_6$)]$^+$), 1101 ([PtAg(Brphen)(tdt)(dppm)]$^+$), 796 ([M − (SbF$_6$)$_2$]$^{2+}$), 666 ([PtAg$_2$(tdt)(dppm)]$^{2+}$). ^{31}P NMR spectrum (202.3 MHz, CD$_3$CN, ppm): δ 5.5 (d, J_{Ag-P} = 436 Hz).

Crystal Structural Determination. Crystals suitable for X-ray diffraction were grown by layering diethyl ether onto the dichloromethane solutions for **1**·$^1/_2$CH$_2$Cl$_2$·$^1/_2$MeOH, **2**·$^3/_2$CH$_2$Cl$_2$, **4**·3CH$_2$Cl$_2$·Et$_2$O·H$_2$O, and **6**·$^3/_2$CH$_2$Cl$_2$·Et$_2$O and by diffusion of diethyl ether into the acetonitrile solutions for **8**·Et$_2$O and **9**·MeCN. Crystallographic parameters and the details for data collections and refinements were summarized in Table 1 for **1**·$^1/_2$CH$_2$Cl$_2$·$^1/_2$MeOH, **2**·$^3/_2$CH$_2$Cl$_2$, and **4**·3CH$_2$Cl$_2$·Et$_2$O·H$_2$O and in Table 2 for **6**·^{3}/2CH$_2$Cl$_2$·Et$_2$O, **8**·Et$_2$O, and **9**·MeCN. Full crystallographic data are provided in the Supporting Information.

Crystals coated with epoxy resin or sealed in capillaries with mother liquors were measured on a SIEMENS SMART CCD diffractometer by ω scan technique at room temperature using graphite-monochromated Mo Kα (λ = 0.71073 Å) radiation. An absorption correction by SADABS was applied to the intensity data.

Table 1. Crystallographic Data for Complexes **1**·$^1/_2$CH$_2$Cl$_2$·$^1/_2$MeOH, **2**·$^3/_2$CH$_2$Cl$_2$, and **4**·3CH$_2$Cl$_2$·Et$_2$O·H$_2$O

	1·$^1/_2$CH$_2$Cl$_2$·$^1/_2$MeOH	**2**·$^3/_2$CH$_2$Cl$_2$	**4**·3CH$_2$Cl$_2$·Et$_2$O·H$_2$O
empirical formula	$C_{83}H_{76}Cl_2Cu_2O_{4.5}P_6PtS_3$	$C_{78.5}H_{69}Cl_5Cu_2N_4O_8P_4PtS_2$	$C_{88}H_{83}Cl_8Cu_2N_4O_{10}P_4PtS_2$
fw	1820.51	1883.8	2150.35
space group	$P2_1/n$	$Pccn$	$P\bar{1}$
a, Å	15.9685(2)	16.0518(7)	13.0050(6)
b, Å	35.9309(7)	16.8922(7)	13.8309(7)
c, Å	16.869(0)	31.7610(13)	28.5804(15)
α, deg			96.380(2)
β, deg	115.341(1)		103.088(1)
γ, deg			106.483(1)
V, Å^3	8747.6(2)	8612.0(6)	4716.1(4)
Z	4	4	2
ρ_{calcd}, g/cm^3	1.382	1.453	1.514
μ, mm^{-1}	2.365	2.440	2.322
radiation (λ, Å)	0.71073	0.71073	0.71073
temp, K	293(2)	293(2)	293(2)
R1(F_o)[a]	0.0826	0.0806	0.0761
wR2(F_o^2)[b]	0.1909	0.1762	0.1775
GOF	1.223	1.243	1.165

[a] $R1 = \sum|F_o - F_c|/\sum F_o$. [b] $wR2 = \sum[w(F_o^2 - F_c^2)_2]/\sum[w(F_o^2)]^{1/2}$.

Scheme 1. Reaction Route of Pt(bpy)(tdt) with $[M_2(dppm)_2(MeCN)_2]^{2+}$ (M = Cu^I or Ag^I) by Self-Assembly

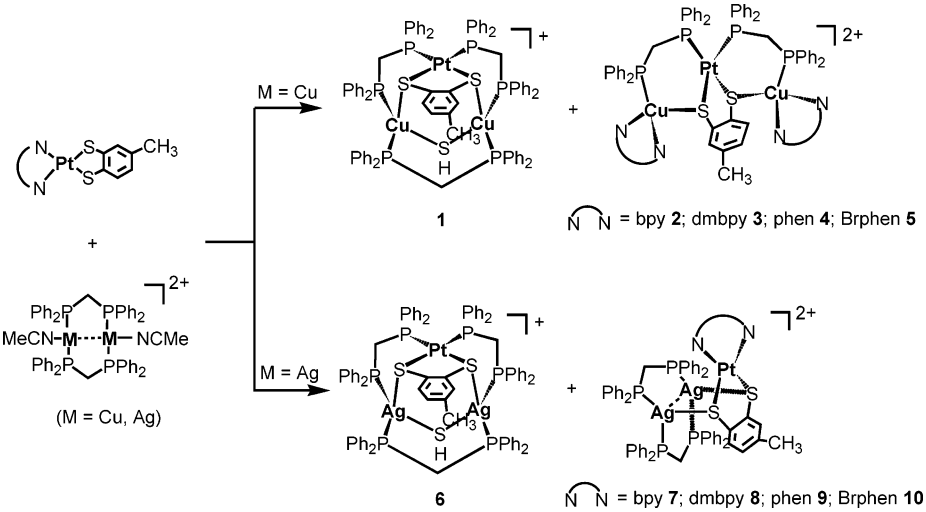

Table 2. Crystallographic Data for Complexes **6**·$^3/_2CH_2Cl_2$·Et_2O, **8**·Et_2O, and **9**·MeCN

	6·$^3/_2CH_2Cl_2$·Et_2O	**8**·Et_2O	**9**·MeCN
empirical formula	$C_{87.5}H_{86}Ag_2Cl_3F_6OP_6PtS_3Sb$	$C_{73}H_{72}Ag_2F_{12}N_2OP_4PtS_2Sb_2$	$C_{71}H_{61}Ag_2F_{12}N_3P_4PtS_2Sb_2$
fw	2188.49	2063.66	2026.56
space group	$P2_1/n$	$P\bar{1}$	$P\bar{1}$
a, Å	16.4509(7)	16.0687(6)	12.9887(2)
b, Å	36.7809(13)	16.1028(6)	14.6457(2)
c, Å	17.3230(8)	19.1188(7)	22.3883(1)
α, deg		86.276(1)	92.106(1)
β, deg	116.685(1)	70.028(1)	106.10(0)
γ, deg		61.534(1)	111.31(0)
V, Å^3	9365.4(7)	4058.6(3)	3766.99(8)
Z	4	2	2
ρ_{calcd}, g/cm^3	1.552	1.689	1.787
μ, mm^{-1}	2.496	3.047	3.281
radiation (*λ*, Å)	0.71073	0.71073	0.71073
temp, K	293(2)	293(2)	293(2)
R1(F_o)[a]	0.0836	0.0888	0.0687
wR2(F_o^2)[b]	0.1774	0.1857	0.1439
GOF	1.248	1.201	1.156

[a] $R1 = \sum|F_o - F_c|/\sum F_o$. [b] $wR2 = \sum[w(F_o^2 - F_c^2)_2]/\sum[w(F_o^2)]^{1/2}$.

The structures were solved by direct method or Patterson procedure, and the heavy atoms were located from E-map. The remaining non-hydrogen atoms were determined from the successive difference Fourier syntheses. All non-hydrogen atoms were refined anisotropically except those mentioned otherwise. The hydrogen atoms were generated geometrically with isotropic thermal parameters. The structures were refined on F^2 by full-matrix least-squares methods using the SHELXTL-97 program package.[26]

The structures were refined by fixing the related bond lengths in the solvate dichloromethane (C−Cl = 1.765 ± 0.005 Å), methanol (C−O = 1.420 ± 0.005 Å), and diethyl ether (C−C = 1.525 ± 0.005 Å, C−O = 1.420 ± 0.005 Å). Isotropic thermal parameters were applied to the non-hydrogen atoms in the solvate molecules. The C−O (1.414 ± 0.005 Å) bond distances of perchlorates were also fixed in the refinement of **1**·$^1/_2CH_2Cl_2$·$^1/_2$MeOH, **2**·$^3/_2CH_2Cl_2$, and **4**·$3CH_2Cl_2$·Et_2O·H_2O. The hydrogen atom of hydroxyl in solvate methanol and those of solvate water were not generated theoretically. Refinement of **1**·$^1/_2CH_2Cl_2$·$^1/_2$MeOH was carried out by fixing the C4−C7 (1.507 ± 0.05 Å) bond length.

(26) Sheldrick, G. M. *SHELXL-97, Program for the Refinement of Crystal Structures*; University of Göttingen: Göttingen, Germany, 1997.

For **2**·$^3/_2CH_2Cl_2$, the oxygen atoms of perchlorates were located in a statistic distribution with the occupancy factors of 0.50 for O1−O4 and O1′−O4′, respectively. The methyl of tdt also exhibited a statistic distribution. For **6**·$^3/_2CH_2Cl_2$·Et_2O, one solvate dichloromethane was disordered, and the Cl atoms (occupancy factors of 0.50 for Cl3, Cl3′, Cl4, and Cl4′, respectively) were located in a statistic distribution. For **8**·Et_2O, one of the silver atoms was located in a statistic distribution with the occupancy factors of 0.90 and 0.10 for Ag2 and Ag2′, respectively. The refinement of **9**·MeCN was performed by assuming a statistic distribution for one of the silver atoms with the occupancy factors of 0.95 and 0.05, respectively, for Ag1 and Ag1′.

Physical Measurements. Elemental analyses (C, H, N) were carried out on a Perkin-Elmer model 240C automatic instrument. Electrospray mass spectra (ES-MS) were recorded on a Finngan LCQ mass spectrometer using dichloromethane−methanol or acetonitrile−methanol as mobile phase. UV−vis absorption spectra in acetonitrile and dichloromethane solutions were measured on a Perkin-Elmer Lambda 25 UV−vis spectrometer. Infrared spectra were recorded on a Magna750 FT-IR spectrophotometer with KBr pellet. ^{31}P NMR spectra were measured on a Varian UNITY-500 spectrometer using 85% H_3PO_4 as external standard. Emission and excitation spectra were recorded on a Perkin-Elmer LS 55 luminescence spectrometer with a red-sensitive photomultiplier type R928. Emission lifetimes were determined on an Edinburgh Analytical Instrument (F900 fluorescence spectrometer) using LED laser at 397 nm excitation, and the resulting emission was detected by a thermoelectrically cooled Hamamatsu R3809 photomultiplier tube. The instrument response function at the excitation wavelength was deconvoluted from the luminescence decay.

Results and Discussion

As shown in Scheme 1, reactions between metal components Pt(diimine)(tdt) and $[M_2(dppm)_2(MeCN)_2]^{2+}$ in an equimolar ratio afforded two types of heterotrinuclear complexes $[PtCu_2(tdt)(\mu\text{-}SH)(dppm)_3](ClO_4)$ (**1**) and $[PtCu_2(diimine)_2(tdt)(dppm)_2](ClO_4)_2$ (diimine = bpy **2**; dmbpy **3**; phen **4**, Brphen **5**) for M = Cu^I, whereas $[PtAg_2(tdt)(\mu\text{-}SH)(dppm)_3](SbF_6)$ (**6**) and $[PtAg_2(diimine)(tdt)(dppm)_2](SbF_6)_2$ (diimine = bpy **7**; dmbpy **8**; phen **9**; Brphen **10**) resulted for M = Ag^I. The pure heterotrinuclear complexes could be separated from each other readily by chromatography on silica gel columns. The combination between Pt(diimine)-

Table 3. Selected Bond Distances (Å) and Angles (deg) for Complexes **1**, **2**, and **4**

1		**2**		**4**	
Pt−S1	2.315(3)	Pt−S	2.302(3)	Pt−S1	2.316(4)
Pt−S2	2.316(3)	Pt−P1	2.289(3)	Pt−S2	2.318(4)
Pt−P2	2.282(3)			Pt−P2	2.302(4)
Pt−P3	2.299(3)			Pt−P4	2.281(4)
Cu1−S1	2.566(3)	Cu−S	2.305(4)	Cu1−N1	2.082(15)
Cu1−S3	2.379(3)	Cu−P2	2.177(4)	Cu1−N2	2.068(13)
Cu1−P1	2.288(3)	Cu−N1	2.058(13)	Cu1−P1	2.183(5)
Cu1−P6	2.289(3)	Cu−N2	2.059(11)	Cu1−S1	2.334(5)
Cu2−S2	2.378(3)			Cu2−N3	2.098(15)
Cu2−S3	2.417(3)			Cu2−N4	2.093(14)
Cu2−P4	2.270(3)			Cu2−P3	2.206(5)
Cu2−P5	2.254(3)			Cu2−S2	2.385(5)
S1−Pt−S2	87.27(10)	S−Pt−S′	86.97(17)	P2−Pt−P4	96.61(14)
S1−Pt−P2	87.38(10)	S−Pt−P1	88.59(11)	S1−Pt−P4	171.72(15)
S1−Pt−P3	171.96(10)	S′-Pt−P1	171.66(11)	S1−Pt−P2	88.85(14)
S2−Pt−P2	174.49(10)	P1−Pt−P1′	96.66(14)	S2−Pt−P4	87.31(14)
S2−Pt−P3	87.38(10)			S2−Pt−P2	172.61(15)
P2−Pt−P3	98.08(10)			S1−Pt−S2	87.96(14)
P1−Cu1−P6	132.28(12)	N2−Cu−N1	78.5(5)	N1−Cu1−N2	80.3(6)
P1−Cu1−S3	108.34(11)	N2−Cu−P2	125.3(3)	P1−Cu1−N1	126.7(4)
P6−Cu1−S3	104.74(12)	N1−Pt−P2	118.5(4)	P1−Cu1−N2	121.9(4)
P1−Cu1−S1	87.67(11)	N2−Pt−S	106.3(3)	S1−Cu1−N1	108.1(5)
P6−Cu1−S1	102.36(11)	N1−Cu−S	105.7(4)	S1−Cu1−N2	106.8(4)
S3−Pt−S1	122.42(11)	P2−Pt−S	115.86(12)	S1−Cu1−P1	109.44(16)
P5−Cu2−P4	137.43(11)			N3−Cu2−N4	79.7(6)
P5−Cu2−S2	107.66(11)			P3−Cu2−N4	131.9(4)
P4−Cu2−S2	96.80(12)			N3−Cu2−P3	118.6(4)
P5−Cu2−S3	101.63(12)			N4−Cu2−S2	97.9(4)
P4−Cu2−S3	97.52(12)			N3−Cu2−S2	107.1(4)
S2−Cu2−S3	116.60(11)			P3−Cu2−S2	115.16(12)
Pt−S1−Cu1	82.74(10)	Pt−S−Cu	103.09(13)	Pt−S1−Cu1	107.74(17)
Pt−S1−C2	103.9(4)	Pt−S−C2	105.9(5)	Pt−S1−C101	104.9(6)
Cu1−S1−C2	105.2(4)	Cu−S−C2	104.2(4)	Cu1−S1−C101	103.0(6)
Pt−S2−Cu2	91.80(11)			Pt−S2−Cu2	96.49(16)
Pt−S2−C1	104.4(4)			Pt−S2−C102	104.5(6)
Cu2−S2−C1	111.2(4)			Cu2−S2−C102	104.3(6)
Cu1−S3−Cu2	92.54(11)				

(tdt) and $[Ag_2(dppm)_2(MeCN)_2](SbF_6)_2$ gives rise to indeed the isolation of the target product $[PtAg_2(diimine)(tdt)(dppm)_2](SbF_6)_2$ (**7**−**10**) and a small amount (yield: ca. 5%) of the unexpected compound **6**. However, self-assembly between Pt(diimine)(tdt) and $[Cu_2(dppm)_2(MeCN)_2](ClO_4)_2$ is carried out by the rearrangement and recombination between the two starting metal components so as to afford heterotrinuclear complexes **1** and $[PtCu_2(diimine)_2(tdt)(dppm)_2](ClO_4)_2$ (**2**−**5**) (Scheme 1). Formation of **1** and **6** results not only from dissociation and recombination of the metal components, but also from disruption of the C−S bonds in the dithiolate (tdt). Rearrangement between metal components Pt(diimine)(tdt) and $[Cu_2(dppm)_2(MeCN)_2](ClO_4)_2$ is likely related to the factors such as different affinity of Pt^{II} and Cu^{I} for the S, P, and N donors, steric requirements, and thermodynamic stability.

The crystal structures of compounds **1**, **2**, **4**, **6**, **8**, and **9** were determined by X-ray diffraction. Selected atomic distances and angles are listed in Table 3 for **1**, **2**, and **4** and in Table 4 for **6**, **8**, and **9**. The perspective views of the coordination cations of **1**, **2**, **6**, and **8** with atom numbering scheme are depicted in Figures 1−4, respectively. The structural drawings of the complex cations of **4** (Figure S1) and **9** (Figure S2) are presented in the Supporting Information.

The dithiolate tdt exhibits a chelating and bridging coordination mode, where it adopts two sulfur donors not only to chelate a Pt^{II} atom, but also to bridge two M^{I} (M = Cu or Ag) atoms, resulting in a heterotrinuclear $PtM_2(tdt)$ (M = Cu for **1**, **2**, and **4**; Ag for **6**, **8**, and **9**) assembly which can exist in two different conformations with *syn* or *anti* form as shown. While the *anti* form is observed in **2** and **4**, the *syn* form occurs in other complexes including **1**, **6**, **8**, and **9**. In both coordination conformations, the coordination plane (S_2P_2 chromophore for **1**, **2**, **4**, and **6**; S_2N_2 chromophore for **8** and **9**) of the Pt^{II} center is almost perpendicular to the plane formed by S_2M_2 (M = Cu or Ag) atoms. For the bridging array Pt−S−M, the chelating Pt−S bond lengths are usually shorter than the bridging M−S distances. Although the bite angles of Pt−S−M (77.58−92.38°) deviate significantly from the ideal value for a sp^3 hybridized sulfur atom except for **2** (103.09°) and **4** (96.49 and 107.74°), the Pt−S−C and M−S−C angles are in the range 96.5−107.0°. The dppm acts as a bridging ligand to link both PtM and M_2 for **1** (M = Cu) and **6** (M = Ag), PtCu for **2** and **4**, or Ag_2 for **8** and **9**. The Pt^{II} centers are located in approximate square-planar environments with S_2P_2 donors for **1**, **2**, **4**, and **6** and S_2N_2 chromophore for **8** and **9**, respectively, whereas the M^{I} atoms provide distorted trigonal-planar (for **8** and **9**) or tetrahedral geometries (**1**, **2**, **4**, and **6**).

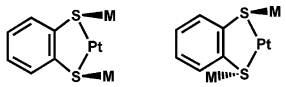

The complex cations $[PtM_2(tdt)(\mu\text{-SH})(dppm)_3]^+$ of **1** (M = Cu, Figure 1) and **6** (M = Ag, Figure 3) contain a chelating and bridging tdt in *syn* conformation, in which Pt^{II}−M^{I} species are also bridged singly by dppm, and the M^{I}−M^{I} atoms are linked by both dppm and sulfhydryl. To our knowledge, **1** and **6** are the sparse examples of $Pt^{II}M^{I}_2$ (M = Cu or Ag) complexes with μ-SH donors as the number of coinage complexes with SH ligands characterized by X-ray crystallography is very limited.[27,28] The Cu−SH (2.379(3) and 2.417(3) Å) bond lengths in **1** are longer than the Cu−S distances observed in the sulfide-bridged Cu^{I} complexes $[Cu_4(dppm)_4(\mu_4\text{−S})](PF_6)_2$[29,30] (2.267−2.268 Å) and $(Ph_4P)_4[Cu_{12}S_8]$ (2.156−2.179 Å),[31] but close to those found in the μ_3-SH capped complex $[Cu_3(Ph_2NHPPh_2)_3(\mu_3\text{−SH})_2](BF_4)$ (2.432−2.518 Å).[28a] The Ag−SH (2.604(4) and 2.632(4) Å) bond lengths in **6** are also longer than the Ag−S distances observed in the sulfide-bridged Ag^{I} complex $[Ag_4(dppm)_4$-

(27) (a) Vicente, J.; Chicote, M.-T.; González-Herrero, P.; Jones, P. G.; Ahrens, B. *Angew. Chem., Int. Ed. Engl.* **1994**, *33*, 1852. (b) Canales, F.; Canales, S.; Crespo, O.; Gimeno, M. C.; Jones, P. G.; Laguna, A. *Organometallics* **1998**, *17*, 1617. (c) Ruiz, J.; Rodríguez, V.; Vicente, C.; Martí, J. M.; López, G.; Pérez, J. *Inorg. Chem.* **2001**, *40*, 5354. (d) Strauch, P.; Dietzsch, W.; Golic, L. *Z. Anorg. Allg. Chem.* **1997**, *623*, 129. (e) Braun, U.; Richter, R.; Sieler, J.; Yanovsky, A. I.; Struchkov, Y. T. *Z. Anorg. Allg. Chem.* **1985**, *529*, 201.
(28) (a) Han, L.; Shi, L. X.; Zhang, L. Y.; Chen, Z. N.; Hong, M. C. *Inorg. Chem. Commun.* **2003**, *6*, 281. (b) Qin, Y. H.; Wu, M. M.; Chen, Z. N. *Acta Crystallogr., Sect. E* **2003**, *59*, m317.
(29) Yam, V. W. W.; Lee, W. K.; Lai, T. K. *Chem. Commun.* **1993**, 1571.
(30) Yang, R. N.; Sun, Y. A.; Hou, Y. M.; Hu, X. Y.; Jin, D. M. *Inorg. Chim. Acta* **2000**, *304*, 1.
(31) Betz, P.; Krebs, B.; Henkel, G. *Angew. Chem., Int. Ed. Engl.* **1984**, *23*, 311.

Table 4. Selected Bond Distances (Å) and Angles (deg) for Complexes **6**, **8**, and **9**

6		**8**		**9**	
Pt−S1	2.319(3)	Pt−S1	2.269(4)	Pt−S1	2.266(3)
Pt−S2	2.310(3)	Pt−S2	2.286(4)	Pt−S2	2.263(3)
Pt−P4	2.304(3)	Pt−N1	2.085(12)	Pt−N1	2.071(10)
Pt−P5	2.325(3)	Pt−N2	2.076(11)	Pt−N2	2.049(10)
Pt−Ag2	3.2865(12)	Ag1−P1	2.519(4)	Ag1−P1	2.477(3)
Ag1−Ag2	3.2629(15)	Ag1−P3	2.452(4)	Ag1−P3	2.455(3)
Ag1−P1	2.417(3)	Ag1−S1	2.684(4)	Ag1−S1	2.638(4)
Ag1−P6	2.467(3)	Ag2−P2	2.516(4)	Ag2−P2	2.514(3)
Ag1−S1	2.648(4)	Ag2−P4	2.489(4)	Ag2−P4	2.464(3)
Ag1−S3	2.632(4)	Ag2−S2	2.669(4)	Ag2−S2	2.679(3)
Ag2−P2	2.480(3)	Ag1−Ag2	2.9309(19)	Ag1−Ag2	2.9567(17)
Ag2−P3	2.497(3)			Pt−Ag2	3.2261(9)
Ag2−S2	2.883(4)				
Ag2−S3	2.606(4)				
P4−Pt−S1	173.72(12)	N1−Pt−N2	78.8(5)	N1−Pt−N2	80.0(4)
P4−Pt−S2	86.63(12)	N2−Pt−S1	173.2(3)	N2−Pt−S1	175.4(3)
S1−Pt−S2	87.09(12)	N1−Pt−S1	95.8(3)	N1−Pt−S1	95.7(3)
P4−Pt−P5	97.42(11)	N2−Pt−S2	97.5(4)	N2−Pt−S2	95.1(3)
S2−Pt−P5	172.55(12)	N1−Pt−S2	176.0(3)	N1−Pt−S2	173.7(3)
S1−Pt−P5	88.80(12)	S1−Pt−S2	88.01(16)	S1−Pt−S2	89.33(11)
P1−Ag1−P6	138.94(12)	P1−Ag1−P3	140.74(14)	P1−Ag1−P3	135.96(12)
P1−Ag1−S3	108.46(12)	P3−Ag1−S1	121.82(13)	P3−Ag1−S1	114.32(12)
P6−Ag1−S3	89.54(12)	P1−Ag1−S1	97.18(13)	P1−Ag1−S1	109.50(12)
P1−Ag1−S1	107.99(11)	P2−Ag2−P4	141.80(14)	P2−Ag2−P4	134.68(9)
P6−Ag1−S1	92.24(12)	P2−Ag2−S2	107.37(14)	P2−Ag2−S2	96.05(9)
S1−Ag1−S3	120.76(11)	P4−Ag2−S2	110.65(14)	P4−Ag2−S2	129.05(9)
P2−Ag2−P3	130.64(12)	Pt−S1−Ag1	89.49(14)	Pt−S1−Ag1	92.38(11)
P2−Ag2−S3	110.57(12)	Pt−S1−C301	104.7(6)	Pt−S1−C1	103.8(4)
P3−Ag2−S3	103.47(12)	Ag1−S1−C301	104.0(6)	Ag1−S1−C1	98.6(4)
P2−Ag2−S2	101.24(11)	Pt−S2−Ag2	91.43(15)	Pt−S2−Ag2	81.03(9)
P3−Ag2−S2	82.90(11)	Pt−S2−C306	103.8(6)	Pt−S2−C2	103.8(4)
S2−Ag2−S3	128.78(11)	Ag2−S2−C306	98.7(5)	Ag2−S2−C2	102.2(4)
Pt−S1−Ag1	90.68(11)				
Pt−S1−C131	105.4(5)				
Ag1−S1−C131	107.0(4)				

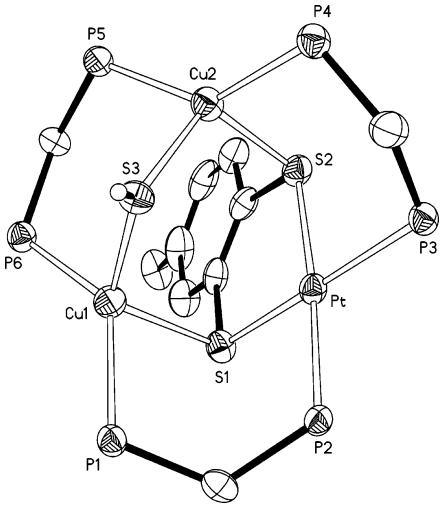

Figure 1. ORTEP drawing of the complex cation of **1** with atom labeling scheme showing 30% thermal ellipsoids. Phenyl rings on the phosphorus atoms are omitted for clarity.

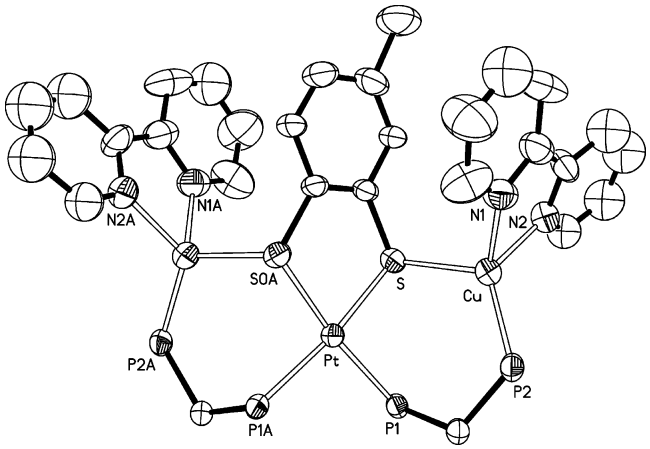

Figure 2. ORTEP drawing of the complex cation of **2** with atom labeling scheme showing 30% thermal ellipsoids. Phenyl rings on the phosphorus atoms are omitted for clarity.

(μ_4-S)](OTf)$_2$ (2.508−2.513 Å),[32] but close to those in [Ag$_3$(dppm)$_3$(μ_3-SH)$_2$](SbF$_6$) (2.661−2.828 Å).[28b] The sulfhydryl (−SH) bridges the Cu^I (for **1**) or Ag^I (for **6**) atoms in an approximately symmetric mode with the bridging angles M−S−M are 92.54(11)° and 77.05(10)° for **1** and **6**, respectively, values which are far from the ideal value for a sp^3 hybridized sulfur atom. The tetrahedrally arranged coordination geometry of the M^I center is built by two P donors from dppm, two S donor from tdt and the sulfhydryl, respectively. The distortion from tetrahedral geometry of M^I center is more severe in **6** (M = Ag) than in **1** (M = Cu). For **1**, the distances from Cu1 and Cu2 to the coordination plane (S1S2P2P3) of the Pt center are 2.483 and 2.420 Å, respectively. The atoms S1 and S2 of tdt are located down the PtCu1Cu2 plane 1.512 and 1.409 Å, respectively, but the atom S3 of sulfhydryl up this plane is 1.605 Å. The Pt···Cu1, Pt···Cu2, and Cu1···Cu2 separations are 3.232, 3.372, and 3.465 Å, respectively. For **6**, the distances from Ag1

(32) Yam, V. W. W.; Lo, K. K. W.; Wang, C. R.; Cheung, K. K. *Inorg. Chem.* **1996**, *35*, 5116.

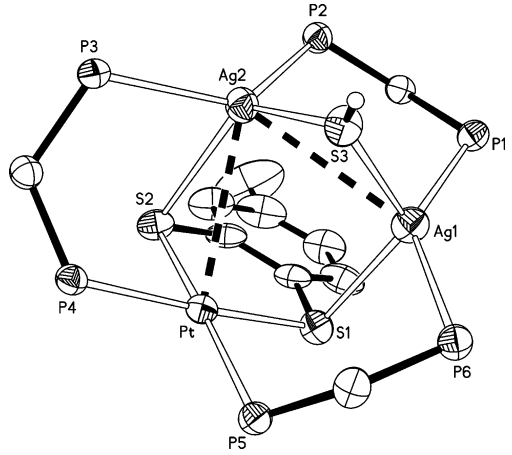

Figure 3. ORTEP drawing of the complex cation of **6** with atom labeling scheme showing 30% thermal ellipsoids. Phenyl rings on the phosphorus atoms are omitted for clarity.

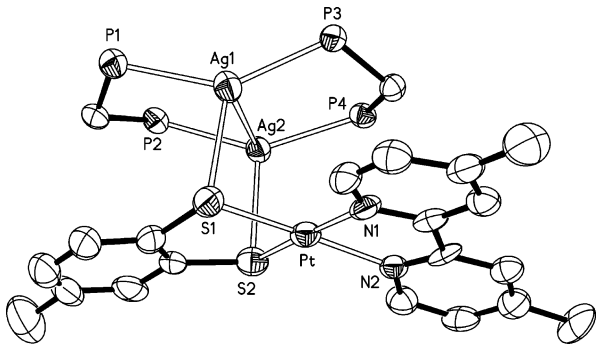

Figure 4. ORTEP drawing of the complex cation of **8** with atom labeling scheme showing 30% thermal ellipsoids. Phenyl rings on the phosphorus atoms are omitted for clarity.

and Ag2 to the coordination plane (S1S2P4P5 atoms) of the Pt center are 2.666 and 2.786 Å, respectively. The atoms S1 and S2 of tdt are located down the PtAg1Ag2 plane by 1.445 and 1.608 Å, respectively, whereas the atom S3 of sulfhydryl is up this plane by 1.982 Å. The Pt···Ag1, Pt···Ag2, and Ag1···Ag2 separations are 3.54, 3.288, and 3.262 Å, respectively.

The dithiolate tdt adopts a chelating and bridging coordination mode in *anti* conformation for **2** (Figure 2) and **4**. The tetrahedral geometry of each Cu^I atom is severely distorted due to the significantly acute chelating angle of bpy or phen with N1−Cu1−N2 and N3−Cu2−N4 angles in the range 78.5(5)−80.3(6)°. The atoms Cu (or Cu1) and CuA (or Cu2) are located down and up the Pt coordination plane 1.894 and 1.894 Å, respectively, for **2**, and 1.819 and 2.121 Å, respectively, for **4**. In **2**, the two 2,2′-bipyridine planes, paralleling to each other, form a dihedral angle of 30.0° with the coordination plane of Pt. In **4**, the planes of 1,10-phenanthroline bound to Cu1 and Cu2 atoms affording a dihedral angle of 31.9° from each other also generate dihedral angles of 31.9° and 11.4°, respectively, with the coordination plane of Pt. The Pt···Cu and Cu1···Cu2 distances are 3.608 and 6.523 Å, respectively, in **2** and 3.507−3.757 and 6.554 Å, respectively, in **4**.

The $PtAg_2$ complex cations in **8** (Figure 4) and **9** consist of binuclear silver component $Ag_2(dppm)_2$ linked by Pt(diimine)(tdt) through the tdt sulfur donors, in which tdt chelates the Pt^{II} center as well as bridges the binuclear silver component in *syn* conformation. The Pt^{II} centers are in approximate square-planar surroundings whereas the Ag^I centers display distorted trigonal-planar geometries. Although the bonding angles (96.1−144.1°) of the Ag^I center deviate severely from 120°, the sum of them is almost 360°, revealing the good planarity of the Ag^I coordination plane. The dihedral angles between the Pt^{II} coordination plane N1N2S1S2 and the plane Ag1Ag2S1S2 are 94.1° and 88.6°, respectively, for **8** and **9**. The distances from Ag1 and Ag2 to the Pt^{II} coordination plane N1N2S1S2 are 2.635 and 2.695 Å for **8**, and 2.673 and 2.612 Å for **9**, respectively. The Ag^I···Ag^I separations for **8** and **9** are 2.932(2) and 2.9567(17) Å, respectively. The platinum···silver distances are 3.499 and 3.558 Å, and 3.226 and 3.539 Å for **8** and **9**, respectively.

ES-MS shows high abundance of molecular positive ion fragments $[M - (ClO_4)]^+$ for **1** and **6**, $[M - (ClO_4)_2]^{2+}$ and $[M - (ClO_4)]^+$ for **2**−**5**, and $[M - (SbF_6)_2]^{2+}$ and $[M - (SbF_6)]^+$ for **7**−**10**. The ^{31}P NMR spectra are characteristic for the heterotrinuclear complexes with variations in structures (see Supporting Information, Figure S3). Typical Pt−P and Ag−P couplings are observed in **1**−**10** with J_{Pt-P} and J_{Ag-P} in the ranges 1450−1570 and 350−450 Hz, respectively. Complex **1** shows Pt^{II} satellites centered at 5.6 ppm with $J_{Pt-P} = 1570$ Hz and two singlets at −11.6 and −17.6 ppm, respectively, ascribed to two types of P donors bonded to Cu^I centers. The counterpart **6** with Ag^I displacing Cu^I in **1** affords a much more complicated ^{31}P NMR spectrum owing to the presence of both Pt−P and Ag−P couplings as well as to partial overlapping of the signals between P donors bound to Pt^{II} and Ag^I centers. For **6**, in addition to typical platinum satellites centered at 6.3 ppm with $J_{Pt-P} = 1450$ and $^2J_{P-P} = 55$ Hz, it gives two set of doublets at −2.5 and −13.6 ppm with $J_{Ag-P} = 439$ and 355 Hz, respectively, due to different types of P donors bound to Ag^I centers. For $PtCu_2$ complexes **2**−**5**, the Pt^{II} satellites occur at ca. 6.9−8.8 ppm with J_{Pt-P} in the range 1457−1517 Hz, whereas the P donors bound to Cu^I centers display one singlet at around −16.0 ppm. The $PtAg_2$ complexes **7**−**10**, however, show only one doublet around 5.0 ppm with $J_{Ag-P} = 427-436$ Hz because of the existence of only one type of P donors bound to Ag^I centers.

Absorption and emission data of complexes **1**−**10** are summarized in Table 5. The electronic absorption spectra of the complexes $[PtM_2(tdt)(\mu\text{-SH})(dppm)_3](ClO_4)$ (M = Cu, **1**; Ag, **6**) in acetonitrile or dichloromethane are characterized by absorption bands at ca. 270 nm together with shoulder bands at ca. 320−350 nm with absorption tail extending to 450 nm. In acetonitrile or dichloromethane solutions, the complexes $[PtCu_2(diimine)_2(tdt)(dppm)_2](ClO_4)_2$ (diimine = bpy **2**; dmbpy **3**; phen **4**; Brphen **5**) show intense high-energy absorption peaks at ca. 230−260 nm with a shoulder at ca. 280−300 nm and low-energy shoulder bands at 355−425 nm with extinction coefficients in the order of 10^3 dm^3 mol^{-1} cm^{-1}. The absorption spectra of $[PtAg_2(diimine)(tdt)(dppm)_2](SbF_6)_2$ (diimine = bpy **7**; dmbpy **8**; phen **9**; Brphen **10**) display intense absorption bands at ca. 230−250 with shoulder peaks at ca. 265−305 and ca. 310−330 nm which

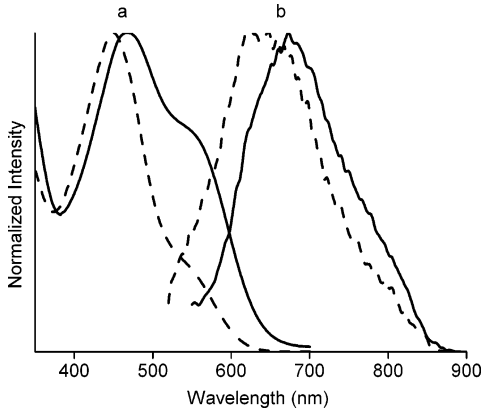

Figure 5. Absorption (a) and emission (b) spectra of **7** (solid line) and **8** (dashed line) in MeCN at 298 K.

Table 5. Absorption and Emission Data for Complexes **1**−**10**

compd	medium	λ_{abs}/nm (ϵ/dm^3 mol^{-1} cm^{-1})	λ_{em}/nm (τ_{em}/μs) at 298 K	λ_{em}/nm at 77 K
1	solid		597 (3.27)	585
	MeCN	277 (28100), 320 (6260)		580
	CH_2Cl_2	273 (36240), 322 (9650)		553
2	solid		607 (0.22)	615
	MeCN	235 (59300), 285 (32640), 360 (5240)		583
	CH_2Cl_2	250 (51700), 294 (35290), 398 (3930)		585
3	solid		593 (0.34)	601
	MeCN	231 (62820), 292 (26660), 351 (5410)		575
	CH_2Cl_2	251 (65400), 293 (37620), 388 (3600)		578
4	solid		591 (0.56)	599
	MeCN	241 (77900), 291 (40740), 408 (5260)		576
	CH_2Cl_2	263 (69200), 287 (59080), 406 (6540)		566
5	solid		606 (0.47)	616
	MeCN	247 (67400), 288 (46550), 415 (4700)		587
	CH_2Cl_2	261 (69500), 287 (45750), 422 (3270)		585
6	solid		605 (2.85)	574
	MeCN	275 (32830), 319 (6110), 347 (4350)		574
	CH_2Cl_2	276 (35080), 318 (5820), 346 (2650)		562
7	solid		593 (4.72)	598
	MeCN	230 (59400), 304 (16060), 328 (6080), 469 (2560), 555 (2120)	673 (<0.1)	602
	CH_2Cl_2	252 (77660), 289 (43560), 327 (13540), 459 (6460)		589
8	solid		571 (2.56)	575
	MeCN	224 (66670), 290 (26820), 325 (7650), 450 (3480), 540 (980)	645 (<0.1)	575
	CH_2Cl_2	246 (65000), 287 (32870), 324 (10320), 445 (4730)		550
9	solid		577 (0.84)	589
	MeCN	243 (91410), 268 (59140), 312 (10450), 458 (4670), 550(2690)	688 (<0.1)	635
	CH_2Cl_2	241 (79950), 267 (66140), 316 (12610), 451 (5130)		587
10	solid		608 (3.65)	613
	MeCN	240 (67470), 275 (49780), 318 (6810), 469 (2240), 565 (1380)	700 (<0.1)	647
	CH_2Cl_2	250 (70570), 275 (61720), 319 (10100), 463 (2940)		618

could be assigned as the origins of ligand-centered transitions. In addition, broad absorption bands of low-energy are observed at ca. 445−465 nm in dichloromethane and at ca. 450−470 nm with a shoulder peak at ca. 540−565 nm in acetonitrile. The low-energy absorption bands are dependent on the electronic properties of substituents in the diimine ligands. By comparison of the low-energy absorption bands of **7** and **8** and those of **9** and **10**, a blue shift from **7** to **8** (Figure 5) as well as a red shift from **9** to **10** are observed. Relative to bpy, the dmbpy species with electron-donating methyl substituents has the effect of raising the energy of the π^*(diimine) and the consequent energy gap, but comparing with phen, Brphen with electron-withdrawing bromo substitutents has the effect of lowering the energy of the π^*-(diimine) and the energy gap. Thus, it is suggested that the low-energy absorption is likely derived from the metal-to-ligand charge transfer (MLCT) [d(Pt)−π^*(diimine)] transition. However, an interligand $\pi \rightarrow \pi^*$ charge transfer (LLCT) from the dithiolate to the diimine ligand could also lead to the observed trend.[15]

With excitation at $\lambda_{ex} > 340$ nm, the complexes [PtM_2-(tdt)(μ-SH)(dppm)$_3$](ClO_4) (M = Cu, **1**; Ag, **6**) show emission in the solid state and in frozen glasses at 77 K. The microsecond range of lifetimes in the solid states at 298 K reveals that the emission is phosphorescent in nature. By comparison of the emission spectrum of **1** with that of **6**, it is observed that the emission energy only shows a slight difference on going from **1** (M = Cu) to **6** (M = Ag) whether in the solid state or in frozen glasses at 77 K. Thus, a possible assignment on the origin of the emitting state bearing chalcogenide-to-metal [SH/dithiolate → M] LMCT character can be excluded.[33] It is likely that the origin of the emission involves an emissive state derived from an MLCT (platinum-to-dithiolate) ^{3}[d(Pt) → $\pi^*_{dithiolate}$] transition as described for mononuclear Pt(dithiolate)(diphosphine) complexes[34] or an LMCT (dithiolate-to-platinum) ^{3}[p(S) → d(Pt)] transition.[35]

The heterotrinuclear complexes [$PtCu_2$(diimine)$_2$(tdt)-(dppm)$_2$](ClO_4)$_2$ (diimine = bpy **2**; dmbpy **3**; phen **4**; Brphen **5**) are nonemissive in fluid solutions but exhibit luminescence in the solid state and in frozen glasses at 77 K with excitation at $\lambda_{ex} > 350$ nm. The microsecond range of lifetimes in the solid state at 298 K is indicative of substantial spin-forbidden character in the emissive state. The emission spectra of **2** and **3** in the solid state at 77 K are presented in Figure S4 (See Supporting Information). In the solid state, while a blue shift of emission energy is observed on going from the bpy complex **2** to the dmbpy counterpart **3**, the emission of the Brphen complex **5** shows a red shift relative to that of the phen counterpart **4**. This is in line with the electron-donating ability of the substituents in diimine ligands, and it is suggested that the emissive origin of **2**−**5** is likely associated with MLCT ^{3}[d(Cu)−π^*(diimine)] transition. However, contribution from MLCT ^{3}[d(Pt) → π^*(dithiolate)] and LLCT [p(S) → π^*(diimine)] transitions cannot be excluded.

Excitation of the complexes [$PtAg_2$(diimine)(tdt)(dppm)$_2$]-(SbF_6)$_2$ (diimine = bpy **7**; dmbpy **8**; phen **9**; Brphen **10**) results in weak emission in fluid acetonitrile solutions, but intense emission in the solid state and in frozen glasses at 77 K. The emissive lifetimes in the microsecond range are suggestive of a triplet state parentage. The emission spectra of **7** and **8** in acetonitrile solutions at 298 K are presented in Figure 5. Excitation bands of **7**−**10** in acetonitrile solutions at 298 K are observed at 340−510 nm, which are close to their low-energy absorption bands, indicative of their similar origin. The emission is therefore tentatively assigned to

(33) Yam, V. W. W.; Lo, K. K. W.; Fung, W. K. M.; Wang, C. R. *Coord. Chem. Rev.* **1998**, *171*, 17.
(34) Bevilacqua, J. M.; Zuleta, J. A.; Eisenberg, R. *Inorg. Chem.* **1994**, *33*, 258.
(35) Yam, V. W. W.; Yu, K. L.; Cheng, E. C. C.; Yeung, P. K. Y.; Cheung, K. K.; Zhu, N. *Chem. Eur. J.* **2002**, *8*, 4122.

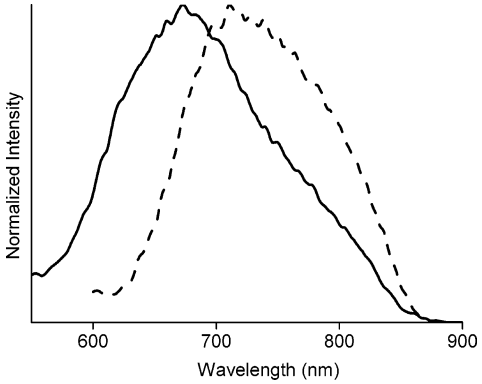

Figure 6. Comparison of the emission spectra of **7** (solid line) and Pt(bpy)(tdt) (dashed line) in MeCN at 298 K.

originate from the triplet state of MLCT ^{3}[d(Pt)/p(S) → π*(diimine)] character.[15] The assignment also coincides with the emission energy trend of **7** < **8** and **9** > **10**, in which electron-donating substitutents in diimine result in a blue shift of emission energy, but a red shift is afforded for electron-withdrawing substitutents. Moreover, compared with emission energies of the corresponding precursor compound Pt(diimine)(tdt),[15a] those of the heterotrinuclear complexes $[PtAg_2(diimine)(tdt)(dppm)_2](SbF_6)_2$ show remarkable blue shifts in fluid acetonitrile solutions ($\Delta E_{em} = 0.10-0.15$ eV) and in the solid state ($\Delta E_{em} = 0.20-0.35$ eV). Figure 6 shows a blue shift of the emission energy of **7** relative to its precursor compound Pt(bpy)(tdt) in acetonitrile solutions at 298 K. This can be elucidated by the bridging character of the tdt S donors to the metal component $[Ag_2(dppm)_2]^{2+}$ which leads to the electronic density of the S donors moving to the Ag^I centers but reduces its flow to the Pt^{II} center, thus lowering the energy of the HOMO and raising the consequent energy gap between HOMO and LUMO. Therefore, incorporation of Pt(diimine)(tdt) to $[Ag_2(dppm)_2]^{2+}$ brings about the raising of the emissive energies of the square planar Pt^{II} diimine chromophores.

Summary

A new synthetic route was established for preparation of a series of heterotrinuclear $Pt^{II}M^I_2$ complexes utilizing luminescent mononuclear compound Pt(diimine)(dithiolate) as synthetic precursor. Incorporation between Pt(diimine)(tdt) and $[M_2(dppm)_2(MeCN)_2]^{2+}$ gives rise to the isolation of three types of novel complexes, i.e., $[PtM_2(tdt)(\mu\text{-SH})(dppm)_3](ClO_4)$ (M = Cu, **1**; Ag, **6**), $[PtCu_2(diimine)_2(tdt)(dppm)_2](ClO_4)_2$ (diimine = bpy **2**; dmbpy **3**; phen **4**, Brphen **5**), and $[PtAg_2(diimine)(tdt)(dppm)_2](SbF_6)_2$ (diimine = bpy **7**; dmbpy **8**; phen **9**; Brphen **10**). The dithiolate tdt affords a μ_3-bonding mode chelating Pt^{II} as well as bridging Cu^I_2 or Ag^I_2 centers in *anti* conformation for $[PtCu_2(diimine)_2(tdt)(dppm)_2](ClO_4)_2$ (**2**−**4**), whereas in *syn* conformation for other complexes. The complexes $[PtAg_2(diimine)(tdt)(dppm)_2](SbF_6)_2$ (**7**−**10**) in fluid solutions at 298 K show low-energy absorption bands due to MLCT [d(Pt) → π*(diimine)] transition. All of the complexes display strong photoluminescence in the solid state and in frozen glasses at 77 K with lifetimes in the microsecond range associated with spin-forbidden triple excited states. The acetonitrile solutions of complexes **7**−**10** afford weak emissions at 298 K, ascribed to the origin of a triplet state of MLCT ^{3}[d(Pt)/p(S) → π*(diimine)] character. Emission energies of the trinuclear heterometallic complexes $[PtAg_2(diimine)(tdt)(dppm)_2](SbF_6)_2$ (**7**−**10**) exhibit a remarkable blue shift (0.10−0.35 eV) relative to those of the precursor compounds Pt(diimine)(tdt). The synthetic approach described herein would afford a significant possibility for developing heterometallic multicomponent systems based on metal diimine components for more efficient photoluminescence and interesting molecular assemblies. Further working is underway in this laboratory.

Acknowledgment. This work was financially supported by NSF of China, NSF of Fujian Province, the fund from Chinese Academy of Sciences, and the national basic research program (001CB108906) from the ministry of sciences and technology of China.

Supporting Information Available: ORTEP drawings of the complex cations of **4** (Figure S1) and **9** (Figure S2); ^{31}P NMR spectra of complexes **1**, **4**, **6** and **9** (Figure S3); emission spectra of **2** and **3** in the solid states at 77 K (Figure S4); and X-ray crystallographic files in CIF format for the structure determinations of compounds **1**·$^1/_2CH_2Cl_2$·$^1/_2$MeOH, **2**·$^3/_2CH_2Cl_2$, **4**·$3CH_2Cl_2$·Et_2O·H_2O, **6**·$^3/_2CH_2Cl_2$·Et_2O, **8**·Et_2O, and **9**·MeCN. This material is available free of charge via the Internet at http://pubs.acs.org.

IC034848A